

New approach to theory of tunneling spectroscopy in unconventional superconductors

A. V. Burmistrova and I. A. Devyatov*

*Lomonosov Moscow State University Skobeltsyn Institute of Nuclear Physics,
1(2), Leninskie gory, GSP-1, Moscow 119991, Russian Federation*

Alexander A. Golubov

*Faculty of Science and Technology and MESA+ Institute of Nanotechnology,
University of Twente, 7500 AE, Enschede, The Netherlands*

Keiji Yada and Yukio Tanaka

*Department of Applied Physics, Nagoya University, Nagoya 464-8603, Japan
(Dated: March 17, 2021)*

We have derived new boundary conditions on wave function at the normal metal / superconductor (NS) interface beyond effective mass approximation. These conditions are based on tight-binding approach and enable one to formulate quantitative model for tunneling spectroscopy of superconductors with complex non-parabolic energy spectra. The model is applied to superconductors with unconventional pairing and with multiband electronic structure. In the case of single band unconventional superconductors this model provides known conductance formula (Phys. Rev. Lett. 74 3451 1995), but with generalized definition of the normal-state conductance. Based on new boundary conditions, we have calculated conductance in normal metal / superconducting pnictide junctions for different orientations of the NS interface with respect to the crystallographic axes of the pnictides. The present approach provides the basis for quantitative tunneling spectroscopy in multi-orbital superconductors.

PACS numbers: 74.20.Rp, 74.70.Xa, 74.45.+c, 74.50.+r, 74.55.+v

I. INTRODUCTION

Tunneling spectroscopy was extensively applied up to now to reveal important features of electronic properties of superconductors.¹ It was predicted long time ago^{2,3} that in a tunnel junction between a normal metal and a metallic BCS superconductor (NS) the differential conductance dI/dV is expressed by the bulk density of states. Later, Blonder, Tinkham and Klapwijk (BTK) formulated the model for dI/dV in NS junctions with arbitrary barrier transparency by solving Bogoliubov-de Gennes (BdG) equation and explicit calculation of the Andreev and normal reflections coefficients.⁴ It was shown that in the regime of low transparency of NS interface the resulting dI/dV corresponds to the energy spectrum of local density of states in a bulk superconductor. On the other hand, dI/dV in high transparency limit is controlled by the Andreev reflection. The original formulation of the BTK theory has provided the basis for tunneling spectroscopy and has been widely applied for many conventional superconducting junctions where the symmetry of superconductor is conventional spin-singlet s -wave. The magnitude of energy gap for conventional s -wave superconductor has been determined with high accuracy. However, the effects of anisotropy of pair potential in d -wave pairing were not included in the original BTK formula. Therefore, after the discovery of high- T_C cuprates, the extension of BTK formula become really needed. Such an extension to unconventional superconductors has been formulated in Refs. 5 and 6. It was shown that tunneling conductance of un-

conventional superconducting junctions is not always expressed by the bulk density of states due to the presence of surface Andreev bound states (ABS).^{6,7} It has been revealed by a theory of tunneling spectroscopy of spin-singlet d -wave superconductor⁶ that zero bias conductance peak (ZBCP) stems from the surface zero energy ABS frequently observed in the experiments of high- T_C cuprates.⁸ This ABS has a flat band dispersion and originates from the sign change of the pair potential on the Fermi surface. Due to this flat dispersion, ZBCP ubiquitously emerges in actual experiments.^{6,7,9} A number of anomalous quantum phenomena like non-monotonic temperature dependence of Josephson current in high T_C cuprate stem from this ABS.¹⁰⁻¹² Further, theory of tunneling spectroscopy of normal metal / spin-triplet p -wave superconductor junctions has been formulated¹³⁻¹⁵ stimulating by the discovery of Sr_2RuO_4 .¹⁶ It was shown that the line shape of a tunneling conductance in chiral p -wave superconducting junctions has a broad ZBCP due to the ABS with linear dispersion.¹⁷⁻¹⁹

At present, to clarify the pairing mechanism of iron-based pnictides is one of hot topics in condensed matter physics. Just after the discovery of superconductivity in pnictides, s_{\pm} symmetry of the pair potential (order parameter) has been proposed,^{20,21} where pair potential changes sign between electron and hole Fermi pockets. The glue of this pairing is provided by spin-fluctuations, which typically appear in strongly correlated superconductors. On the other hand, s_{++} -wave pairing symmetry due to orbital fluctuations has been proposed as another candidate of superconducting pairing.²² The pos-

sibility of the inter-orbital pairing was also discussed.²³ Since iron pnictides are multi-orbital systems with multiple orbital systems, a theory of tunneling spectroscopy applicable to multi-orbital superconductors is strongly needed. Besides pnictides, there are many new unconventional superconductors with multiple Fermi surfaces such as doped topological insulator $\text{Cu}_x\text{Bi}_2\text{Se}_3$.^{24–32}

However, formulation of microscopic theory of tunneling spectroscopy in multi-band superconductors is highly nontrivial task. The most crucial point is the boundary conditions on wave functions at the NS interface. Araújo and Sacramento have presented a new way to describe boundary conditions between single-band normal metal and multi-band superconducting systems using phenomenological approach based on analogy between quantum waveguide theory and interband scattering.³³ This idea was applied to actual pnictide junctions,^{33,34} but the basis of this theory is not fully microscopic since interband and intervalley scattering effect is not fully taken into account. Other theories devoted to the study of coherent transport in junctions of iron pnictides are also phenomenological.^{35–41} The formulation of boundary conditions on the wave function in multi-band systems has not become clear up to now.

In this paper, based on equations of tight-binding model, we obtain the boundary conditions on the wave functions for the contact between a normal metal and a multiband superconductor. Up to now, tight-binding approach has been used for the study of ABS in various superconductors.^{42–48} Here, we obtain boundary conditions beyond the effective mass approximation in order to take into account complex nonparabolic and anisotropic spectrum of energy band in the normal state and unconventional pairing in multi-band superconducting systems. The obtained boundary conditions provide an extension of tight-binding approach by Zhu and Kroemer⁴⁹ to a superconducting case. The approach⁴⁹ is physically transparent, since the only assumption is the prolongation of solutions of tight-binding model on one additional site to the left (right) sides of an interface. We apply the derived boundary conditions to the calculation of charge conductance between a normal metal and an iron pnictide superconductor for different misorientation angles between crystallographic axes of a pnictide superconductor and the interface. Application of our theory to single band unconventional superconducting junctions allows one to reproduce preexisting formula of tunneling spectroscopy of unconventional superconductors, where the transparency of the junction in the normal state has a different momentum dependence. Brief account of some results of this paper is given in Ref. 50.

II. ONE-DIMENSIONAL MODEL

In order to understand the essence of new boundary conditions, we first consider one-dimensional model of normal metal and spin-singlet s -wave superconductor

junction. We use a model Hamiltonian H of the 1D chain of atoms, whose electronic states are described in the tight-binding approximation, where Cooper pair is formed on the same site:

$$H = H_N + H_S + H_I, \quad (1)$$

$$H_N = \sum_{n \leq 0, \sigma} \left[t' \left(a_{\sigma, n-1}^\dagger a_{\sigma, n} + h.c. \right) - \mu_N a_{\sigma, n}^\dagger a_{\sigma, n} \right], \quad (2)$$

$$H_S = \sum_{n \geq 1, \sigma} \left[t \left(a_{\sigma, n}^\dagger a_{\sigma, n+1} + h.c. \right) - \mu_S a_{\sigma, n}^\dagger a_{\sigma, n} \right] - \sum_n \left[\Delta a_{\uparrow, n}^\dagger a_{\downarrow, n}^\dagger + h.c. \right], \quad (3)$$

$$H_I = \gamma \left(a_{\sigma, 0}^\dagger a_{\sigma, 1} + h.c. \right), \quad (4)$$

with creation (annihilation) operator $a_{\sigma, n}^\dagger$ ($a_{\sigma, n}$) of an electron with spin σ on n site, and pair potential Δ . t' (t) and μ_S (μ_N) are hopping and chemical potential in normal metal (superconductor), respectively. H_N , H_S and H_I are hamiltonian in the normal metal (N), in the superconductor (S) and at the interface, respectively. Eq. (1) is diagonalized by introducing the following canonical transformation:

$$a_{\sigma, n} = \sum_\nu \left[u_{\nu, n} \alpha_{\nu, \sigma} + \text{sgn}(\sigma) v_{\nu, n}^* \alpha_{\nu, -\sigma}^\dagger \right], \quad (5)$$

which is a generalization of the Bogoliubov transformation⁵¹ to the case of a discrete lattice. In Eq. (5) $\alpha_{\nu, -\sigma}^\dagger$ ($\alpha_{\nu, \sigma}$) are operators of creation (annihilation) of quasiparticles satisfying Fermi anti-commutation relations, and $u_{\nu, n}$, $v_{\nu, n}$ are wave functions in BdG equation. The discrete version of BdG equations for wave functions $u_{\nu, n}$, $v_{\nu, n}$ has the form:

$$\begin{cases} t_n u_{\nu, n+1} + t_{n-1} u_{\nu, n-1} - \mu_n u_{\nu, n} \\ + \Delta_n v_{\nu, n} = \varepsilon_\nu u_{\nu, n}, \\ t_n v_{\nu, n+1} + t_{n-1} v_{\nu, n-1} - \mu_n u_{\nu, n} \\ - \Delta_n^* u_{\nu, n} = -\varepsilon_\nu v_{\nu, n}, \end{cases} \quad (6)$$

where $\mu_n = \mu_N$ (μ_S) for $n \leq 0$ ($n \geq 1$), and $t_n = t'$, γ and t for $n \leq -1$, $n = 0$ and $n \geq 1$, respectively. Basically, Eq. (6), together with the corresponding self-consistent equations for the pair potential Δ_n , provides the description for any spatially-inhomogeneous problem with an arbitrary set of hopping parameters between sites t_n . However, this problem can be solved only numerically. In order to formulate a relevant simplified model for an NS junction which allows analytical solution, we assume that there is no inhomogeneity of pair potential in a superconductor. That means, $\Delta_n = \Delta$ for $n \geq 1$ and

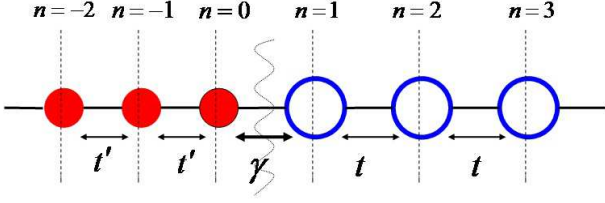


FIG. 1. Schematic illustration of one-dimensional model. Left region (red filled circles) corresponds to that of normal metal with hopping parameter t' , right region (blue circles) corresponds to that of superconductor with hopping parameter t . The hopping parameter at NS boundary is given by γ .

$\Delta_n = 0$ for $n \leq 0$. The structure under consideration is depicted in Fig. 1.

First, we consider the conductance in a normal metal / normal metal junction by setting $\Delta = 0$ in a superconducting region. The electron with energy $E (= \varepsilon_\nu)$ is injected from the left side and it is scattered at the interface. Then the wave functions $u_{\nu,n}$ for the left side $\Phi_n (= u_{\nu,n})$ with $n \leq 0$ and the right side $\Psi_n (= u_{\nu,n})$ with $n \geq 1$ are given by

$$\begin{cases} \Phi_n = \exp(iqnl) + b \exp(-iqnl), \\ \Psi_n = c \exp(iknl), \end{cases} \quad (7)$$

where l is the lattice constant in a normal metal and a superconductor (for clarity, we consider them to be equal, but this restriction is not required.⁴⁹) The first and the second term of Φ_n represent an incident and a normal reflected waves, respectively. Ψ_n corresponds to a transmitted wave. Here, q and k are determined by the equation $2t' \cos(ql) = \mu_N + E$ and $2t \cos(kl) = \mu_S + E$ with $q, k \geq 0$, respectively. The coefficients b and c are determined by the boundary conditions. These boundary conditions were proposed by Zhu and Kroemer.⁴⁹ Their method is not limited by the assumption of parabolic single-particle excitation spectrum based on the electronic effective-mass concept. In their idea, one can obtain the boundary conditions by the shift of the location of the boundary. If we shift the boundary to the right, we obtain the Shrödinger equation

$$E\Phi_0 = -\mu_N\Phi_0 + t'\Phi_{-1} + t'\Phi_1, \quad (8)$$

where Φ_1 is obtained by the natural extension of Φ_n ($n \leq 0$) given in Eq. (7). The Shrödinger equation without the shift of the boundary is given by

$$E\Phi_0 = -\mu_N\Phi_0 + t'\Phi_{-1} + \gamma\Psi_1. \quad (9)$$

By subtracting Eq. (8) from Eq. (9), we obtain the boundary condition

$$t'\Phi_1 = \gamma\Psi_1. \quad (10)$$

Similarly, if we shift the boundary to the left, we obtain the boundary condition

$$\gamma\Phi_0 = t\Psi_0. \quad (11)$$

Using the boundary conditions Eqs. (10) and (11) and the wave functions Eq. (7), one can obtain b, c given in Eq. (7):

$$b = \frac{\sigma_1 \exp(iql) - \exp(ikl)}{\exp(ikl) - \sigma_1 \exp(-iql)},$$

$$c = \gamma(1+b)/t, \quad (12)$$

with $\sigma_1 = tt'/\gamma^2$, and expression for the transparency σ_N at the interface:

$$\sigma_N(k, q) = 1 - |b|^2 = \frac{2\sigma_1 [\cos[(q-k)l] - \cos[(q+k)l]]}{1 + \sigma_1^2 - 2\sigma_1 \cos[(q+k)l]}. \quad (13)$$

The boundary conditions Eqs. (10) and (11) provide the conservation of probability flow J across the interface:

$$J_{n \leq -1} = \frac{2t'}{\hbar} \text{Im}(\Phi_{n+1}^* \Phi_n) = J_{n > 1} = \frac{2t}{\hbar} \text{Im}(\Psi_{n+1}^* \Psi_n). \quad (14)$$

After introducing finite difference derivatives in the following form: $\psi'_1 = (\Psi_1 - \Psi_0)/l$, $\psi'_2 = (\Phi_1 - \Phi_0)/l$, the boundary conditions Eqs. (10) and (11) lead to usual boundary conditions,⁵² obtained early in the continuum limit. It is necessary to note that these boundary conditions, written in the form of finite differences, coincide with the mostly used Harrison's boundary conditions⁵³ only for the case $\sigma_1 = 1$. This feature of discrete boundary conditions Eqs. (10) and (11) were also mentioned in Ref. 49.

By extending the method⁴⁹ to the case of superconducting junctions, one can obtain from Eq. (6) the following four boundary conditions at the interface between normal metal and spin-singlet s -wave superconductor junctions (see Fig. 1):

$$\begin{cases} t'\Phi_1 = \gamma\Psi_1, \\ t'\bar{\Phi}_1 = \gamma\bar{\Psi}_1, \\ \gamma\Phi_0 = t\Psi_0, \\ \gamma\bar{\Phi}_0 = t\bar{\Psi}_0, \end{cases} \quad (15)$$

where $\Psi_n(\Phi_n)$ and $\bar{\Psi}_n(\bar{\Phi}_n)$ are the wave functions $u_{\nu,n}$ and $v_{\nu,n}$ for electron and hole in S (N), respectively. These wave functions are given by

$$\begin{cases} \Phi_n = \exp(iqnl) + b \exp(-iqnl), \\ \bar{\Phi}_n = a \exp(i\tilde{q}nl), \\ \Psi_n = c u \exp(iknl) + d v \exp(-i\tilde{k}nl), \\ \bar{\Psi}_n = c v \exp(iknl) + d u \exp(-i\tilde{k}nl). \end{cases} \quad (16)$$

The wave functions of a normal metal and a superconductor contain four unknowns a, b, c, d describing the

Andreev and normal reflected waves in a normal metal, and two transmitted waves in the superconductor (c and d), where c (d) corresponds to transmission process by electron-like (hole-like) quasiparticles. These four unknowns (a, b, c, d) are uniquely defined by four boundary conditions Eq. (15). In Eq. (16), q, \tilde{q} (k, \tilde{k}) are wave vectors in normal metal (superconductor), corresponding to the energy E .

Although q and \tilde{q} are real numbers, k and \tilde{k} become complex when $|E| < |\Delta|$ is satisfied. One can show that obtained wave functions provide the conservation of the probability flow by postulating boundary conditions Eq. (15). The expression for the probability flow on a discrete lattice (Fig. 1) follows from the BdG equations on the sites of the crystal lattice Eq. (6):

$$J_s = \frac{2}{\hbar} \text{Im}(t\Psi_{n+1}^* \Psi_n - t\bar{\Psi}_{n+1}^* \bar{\Psi}_n). \quad (17)$$

It is necessary to note that the condition for the conservation of probability flow at the interface between N and S, having the form of discrete sums (differences) in the crystal lattice (Eqs. (14), (17)), can be written in a quadratic form in terms of the probability amplitudes to be in states with wave vectors $q, -q, \tilde{q}, k, -\tilde{k}$ multiplied on the group velocities in these states:

$$\begin{aligned} \frac{\partial \varepsilon_n}{\partial p} \Big|_{p=q} - |a|^2 \frac{\partial \varepsilon_n}{\partial p} \Big|_{p=\tilde{q}} + |b|^2 \frac{\partial \varepsilon_n}{\partial p} \Big|_{p=-q} = |c|^2 \frac{\partial \varepsilon_s}{\partial p} \Big|_{p=k} \\ + |d|^2 \frac{\partial \varepsilon_s}{\partial p} \Big|_{p=-\tilde{k}}. \end{aligned} \quad (18)$$

Eq. (18) is similar to the corresponding expression in Ref. 4.

The above consideration of the tight-binding approximation of one-dimensional model of the NS junctions corresponds to equilibrium situation with zero voltage at the boundary $V = 0$. However, it can be generalized to the case of a finite voltage $V \neq 0$ on the microconstriction of atomic sizes with a characteristic size much smaller than the elastic l_{el} and inelastic l_{in} characteristic mean free paths. In such pure microconstriction electron transport can be considered as a transport on the independent transverse modes. The current flowing through one mode is determined by the difference between the incoming $f^{\rightarrow}(E)$ and outgoing $f^{\leftarrow}(E)$ flows of electrons in the normal metal:⁴

$$I(V) = \eta_1 \int \{f^{\rightarrow}(E) - f^{\leftarrow}(E)\} dE, \quad (19)$$

where $f^{\rightarrow}(E) = f_0(E - eV)$, $f_0(E)$ - the equilibrium Fermi distribution, $\eta_1 = e/(\pi\hbar)$, and

$$\begin{aligned} f^{\leftarrow}(E) = A(E)(1 - f^{\rightarrow}(-E)) + B(E)f^{\rightarrow}(E) \\ + (C(E) + D(E))f_0(E). \end{aligned} \quad (20)$$

In Eq. (20) $A(E)$, $B(E)$, $C(E)$ and $D(E)$ are probabilities of the Andreev reflection, normal reflection, transmission as a electron-like quasiparticle and as a hole-like quasiparticle, respectively. The probabilities A, B, C, D in Eq. (20) are calculated from the boundary conditions Eq. (15) and the expressions for the probability flow Eqs. (14), (17). In calculating the probabilities A, B, C, D the incoming quasiparticle states must be normalized so that the probability flow in these states, described by the Eqs. (14), (17), is equal to unity. This normalization provides a thermodynamic equilibrium in the absence of voltage $V = 0$ on the NS junction.

For the majority of superconductors, the magnitudes of Δ and E are much smaller than those of t and t' and the following conditions

$$|\Delta/t| \ll 1, |\Delta/t'| \ll 1 \quad (21)$$

are satisfied. This is the so-called quasiclassical approximation. Then, the relations $q \simeq \tilde{q} \simeq q_0$ and $k \simeq \tilde{k} \simeq k_0$ are satisfied, where k_0 and q_0 are momenta at the Fermi surface satisfying $2t' \cos(q_0 l) = \mu_N$ and $2t \cos(k_0 l) = \mu_S$. The resulting amplitudes a and b are given by

$$\begin{aligned} a = \frac{2\sigma_1 \Gamma (\cos[(q_0 - k_0)l] - \cos[(q_0 + k_0)l])}{\Lambda}, \\ b = \frac{(1 - \frac{\delta\sigma_+}{\delta})(1 - \frac{\sigma_+}{\delta\delta})}{\Lambda} \end{aligned} \quad (22)$$

with

$$\Gamma = \Delta / (E + \sqrt{E^2 - \Delta^2}), \exp(iq_0 l) = \delta, \exp(ik_0 l) = \tilde{\delta} \text{ and}$$

$$\Lambda = -(1 - \sigma_1 \delta \tilde{\delta})(1 - \sigma_1 \frac{1}{\delta \tilde{\delta}})[1 - (1 - \sigma_N(k_0, q_0)\Gamma^2)],$$

where $\sigma_N(k_0, q_0)$ is defined by Eq. (13)

Within this approximation, we can reproduce the BTK result⁴

$$I(V) = \eta_1 \int \{f_0(E - eV) - f_0(E)\} \sigma(E) dE, \quad (23)$$

where

$$\begin{aligned} \sigma(E) = 1 + |a|^2 - |b|^2 \\ = \frac{\sigma_N [1 + \sigma_N |\Gamma|^2 + (\sigma_N - 1) |\Gamma|^4]}{|1 - (1 - \sigma_N)\Gamma^2|^2}. \end{aligned} \quad (24)$$

This is the well-known formula⁴ with extended definition of the transparency σ_N (see Eq. (13)) at the N/S interface.

In this section, we have studied one-dimensional model with spin-singlet s -wave superconductor as the simplest case. However, the case of the contact between a normal metal and a superconductor with anisotropic sign-changing pair potential on the Fermi surface is of most interest. The next two sections will be devoted to the consideration of this situation.

III. TWO-DIMENSIONAL MODEL FOR THE CONTACT OF A NORMAL METAL AND D-WAVE SINGLE BAND SUPERCONDUCTOR

In this section, we extend our approach to unconventional superconductor. We show one typical example of two-dimensional lattice model of unconventional superconductor. BdG equations on sites of the lattice of the d -wave superconductor in the $x - y$ plane have the following form:

$$\left\{ \begin{array}{l} t_1(\Psi_{n+1,m} + \Psi_{n-1,m}) \\ + t_2(\Psi_{n,m+1} + \Psi_{n,m-1}) - \mu_S \Psi_{n,m} \\ + \Delta_0(\bar{\Psi}_{n+1,m} + \bar{\Psi}_{n-1,m} - \bar{\Psi}_{n,m+1} - \bar{\Psi}_{n,m-1}) \\ = \varepsilon \Psi_{n,m}, \\ t_1(\bar{\Psi}_{n+1,m} + \bar{\Psi}_{n-1,m}) \\ + t_2(\bar{\Psi}_{n,m+1} + \bar{\Psi}_{n,m-1}) - \mu_S \bar{\Psi}_{n,m} \\ - \Delta_0(\Psi_{n+1,m} + \Psi_{n-1,m} - \Psi_{n,m+1} - \Psi_{n,m-1}) \\ = -\varepsilon \bar{\Psi}_{n,m}, \end{array} \right. \quad (25)$$

where t_1, t_2 are hopping amplitudes between orbitals on sites, n, m are the numbers of site in x - and y -direction, respectively. The value of Δ_0 is the amplitude of the anisotropic pair potential corresponding to the considered d -wave superconducting pairing: $\Delta(k) = 2\Delta_0(\cos k_x - \cos k_y)$, where k_x and k_y is quasimomentum perpendicular and parallel to the interface, respectively.

The boundary conditions for the contact of a normal metal and d -wave superconductor, described by the Eq. (25), in the quasiclassical limit Eq. (21) are the same as boundary conditions Eq. (15). For the case under consideration, Ψ_n ($\bar{\Psi}_n$) in boundary conditions Eq. (15) means the wave function of layer n of atoms of d -wave superconductor in the $x - y$ plane. Due to the translational symmetry in the y -direction in the electron (hole) wave functions $\Psi_{n,m}$ ($\bar{\Psi}_{n,m}$) we can omit second subscript (m) corresponding to the coordinate of an atom in a direction parallel to the boundary. It should be remarked that within quasiclassical approximation, these boundary conditions are satisfied for any type of unconventional superconductors.

Let's consider the situation, when the misorientation angle between interface and crystallographic axes of superconductor is equal to $\pi/4$. In this case the current through the two-dimensional pure microconstriction between a normal metal and d -wave superconductor is determined by the integration over the transverse quasimomentum k_y of Eq. (23): $I_p(V) = \eta_2 \int dk_y I(V, k_y)$, where $\eta_2 = \Xi/2\pi$, Ξ - characteristic size of microconstriction, with the following definition of $\sigma(E)$:

$$\sigma(E) = \frac{\sigma_N[1 + \sigma_N |\Gamma|^2 + (\sigma_N - 1) |\Gamma\tilde{\Gamma}|^2]}{|1 - (1 - \sigma_N)\Gamma\tilde{\Gamma}|^2}, \quad (26)$$

with $\Gamma = \Delta_+/(E + \sqrt{E^2 - \Delta_+^2})$ and $\tilde{\Gamma} = \Delta_-/(E +$

$\sqrt{E^2 - \Delta_-^2})$ with $\Delta_{\pm} = \Delta(\pm k_x, k_y)$.

The present result is nothing but the formula of unconventional tunneling conductance by Tanaka and Kashiwaya^{6,7,54} with generalized definition of σ_N , presented by Eq. (13). The surface ABS is generated when the denominator of $\sigma(E)$ becomes zero for $\sigma_N = 0$. This condition is given by

$$1 = \Gamma\tilde{\Gamma}.$$

Here, we consider d_{xy} -wave pairing with $\Delta_+ = -\Delta_- = 4\Delta_0 \sin k_x \sin k_y$. After simple manipulation, the energy level of surface ABS becomes $E = 0$ for any k_y on the Fermi surface. The dispersionless surface ABS is generated in this case. The topological origin of this flat band ABS has been clarified recently.^{55,56}

IV. TWO-DIMENSIONAL MODEL FOR THE CONTACT OF A NORMAL METAL AND A TWO BAND SUPERCONDUCTING Pnictide

A. Zero misorientation angle

Consider the application of this method for the case of two-dimensional electron transport through the boundary of a normal metal and a superconducting pnictide. In superconducting pnictides, there are two kinds of Fermi surfaces. One is the hole-like Fermi surface around Γ -point, and the other is the electron-like Fermi surface around the zone boundary. The minimum model to reproduce these Fermi surfaces is two-band model considering the d_{zx} and d_{yz} orbitals in iron $3d$ -orbitals.⁵⁷ In this model, there are four kinds of hopping parameters t_1, t_2, t_3 and t_4 . As shown in Fig. 2, t_1 (t_2) is the intra-orbital hopping between d_{zx} (d_{yz})-orbitals in nearest neighbor site, t_3 and t_4 are intra-orbital and inter-orbital hopping between next nearest neighbor sites, respectively. For the pair potential, s_{\pm} model with $\Delta = 4\Delta_0 \cos k_x \cos k_y$ and s_{++} model with $\Delta = 2\Delta_0(\cos k_x + \cos k_y) + \Delta_1$ are proposed.^{57,58} These pair potentials correspond to intra-orbital pairing and do not depend on the type of orbital.

Let us first study the case of zero misorientation angle of the crystallographic axes of a pnictide with respect to the interface as shown in Fig. 2. The hopping perpendicular and oblique hopping between the sites on the left side and d_{zx} (d_{yz})-orbitals on the right side are described by γ_1 (γ_2) and $\gamma'_1, \gamma''_1, (\gamma'_2, \gamma''_2)$, respectively. For simplicity, we assume that the periods of the crystal lattices in a normal metal and a pnictide are the same. In the following calculations, we drop oblique hopping for simplicity. The mathematical formulation of the problem and solutions of BdG equations in the two-dimensional case are given in Appendix.

Proceeding as well as in the derivation of boundary conditions in the 1D-model Eq. (15), but taking into account independent hopping on d_{xz} and d_{yz} -orbitals of a pnictide, we obtain the following boundary conditions for NS junction with zero misorientation angle:

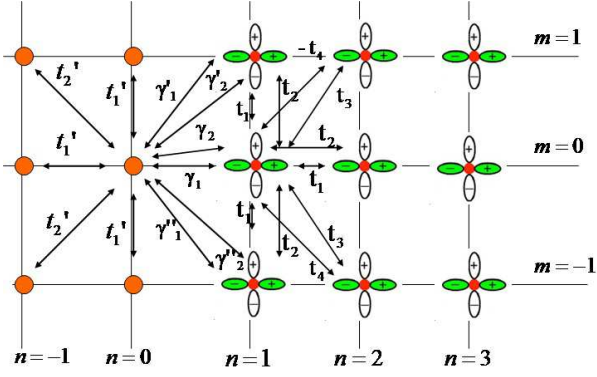


FIG. 2. Boundary of normal metal / superconducting pnictide junction without misorientation. Left region (orange circles) corresponds to the region of normal metal with hopping parameter t'_1, t'_2 , right region (sites with two d -orbitals) corresponds to the region of a superconducting pnictide with hopping parameters t_1, t_2, t_3, t_4 . γ_1 (γ_2) and γ'_1 (γ'_2) are perpendicular and oblique hopping across the boundary to d_{xz} (d_{yz})-orbitals of a pnictide, respectively.

$$\left\{ \begin{array}{l} t'_1 \Phi_1 = \gamma_1 \Psi_1^\alpha + \gamma_2 \Psi_1^\beta, \\ t'_1 \bar{\Phi}_1 = \gamma_1 \bar{\Psi}_1^\alpha + \gamma_2 \bar{\Psi}_1^\beta, \\ \gamma_1 \Phi_0 = (t_1 + 2t_3 \cos k_y) \Psi_0^\alpha + 2it_4 \sin k_y \Psi_0^\beta \\ + 2\Delta_0 \zeta(k_y) \bar{\Psi}_0^\alpha, \\ \gamma_1 \bar{\Phi}_0 = (t_1 + 2t_3 \cos k_y) \bar{\Psi}_0^\alpha + 2it_4 \sin k_y \bar{\Psi}_0^\beta \\ - 2\Delta_0 \zeta(k_y) \Psi_0^\alpha, \\ \gamma_2 \Phi_0 = (t_2 + 2t_3 \cos k_y) \Psi_0^\beta + 2it_4 \sin k_y \Psi_0^\alpha \\ + 2\Delta_0 \zeta(k_y) \bar{\Psi}_0^\beta, \\ \gamma_2 \bar{\Phi}_0 = (t_2 + 2t_3 \cos k_y) \bar{\Psi}_0^\beta + 2it_4 \sin k_y \bar{\Psi}_0^\alpha \\ - 2\Delta_0 \zeta(k_y) \Psi_0^\beta, \end{array} \right. \quad (27)$$

where $\zeta(k_y) = \cos k_y$ and $1/2$ for s_\pm and s_{++} models, respectively. Due to the translational symmetry of this structure in a direction parallel to the boundary, k_y component of the quasimomentum is conserved. Also because of this translational symmetry in the electron (hole) wave functions $\Psi_{n,m}^{\alpha(\beta)}$ ($\bar{\Psi}_{n,m}^{\alpha(\beta)}$), the second subscript (m) corresponding to the coordinate of an atom in a direction parallel to the boundary is omitted. The wave functions of the NS contact are defined by 6 plane waves with amplitudes a, b, c_1, c_2, d_1, d_2 : a, b describe the Andreev and normal reflected waves in normal metal. c_1 (c_2) and d_1 (d_2) describe electron-like and hole-like transmitted waves corresponding to inner (outer) Fermi surface in a superconducting pnictide, respectively:

$$\left\{ \begin{array}{l} \Phi_n = \exp(iq_1 nl) + b \exp(-iq_1 nl), \\ \bar{\Phi}_n = a \exp(iq_2 nl), \\ \Psi_n^\alpha = c_1 u_1(k_1) \exp(ik_1 nl) + c_2 u_1(k_2) \exp(ik_2 nl) \\ + d_1 u_1(k_3) \exp(ik_3 nl) + d_2 u_1(k_4) \exp(ik_4 nl), \\ \Psi_n^\beta = c_1 u_2(k_1) \exp(ik_1 nl) + c_2 u_2(k_2) \exp(ik_2 nl) \\ + d_1 u_2(k_3) \exp(ik_3 nl) + d_2 u_2(k_4) \exp(ik_4 nl), \\ \bar{\Psi}_n^\alpha = c_1 v_1(k_1) \exp(ik_1 nl) + c_2 v_1(k_2) \exp(ik_2 nl) \\ + d_1 v_1(k_3) \exp(ik_3 nl) + d_2 v_1(k_4) \exp(ik_4 nl), \\ \bar{\Psi}_n^\beta = c_1 v_2(k_1) \exp(ik_1 nl) + c_2 v_2(k_2) \exp(ik_2 nl) \\ + d_1 v_2(k_3) \exp(ik_3 nl) + d_2 v_2(k_4) \exp(ik_4 nl). \end{array} \right. \quad (28)$$

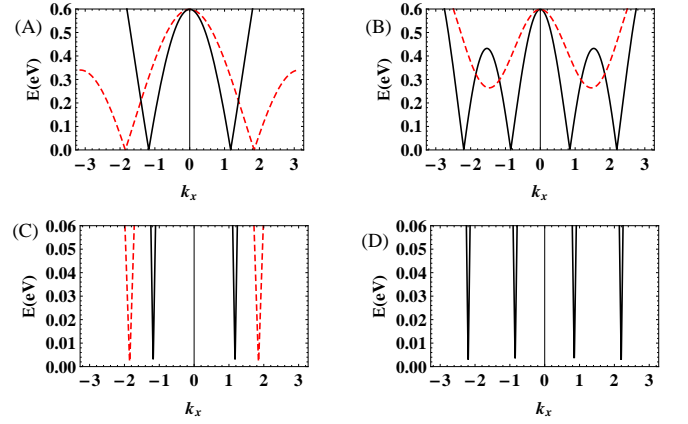


FIG. 3. The excitation spectrum of a superconducting pnictide for a fixed value of k_y . (A) - misorientation angle is equal to 0, $k_y = 0$, (B) - misorientation angle is equal to $\pi/4$, $k_y = 0$, (C) corresponds to the (A), depicted on a larger scale, (D) corresponds to (B), depicted on a larger scale. Red dashed line and black solid line correspond to the two different bands.

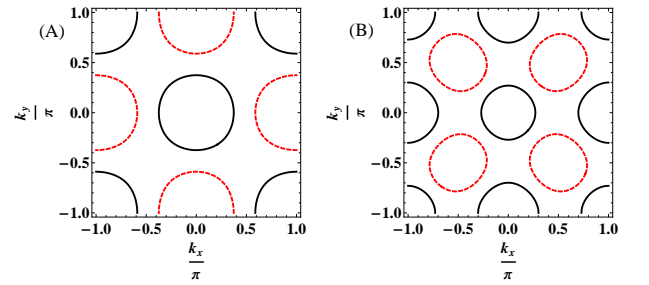


FIG. 4. The Fermi surface of a pnictide in the unfolded Brillouin zone. (A) - misorientation angle is equal to 0, (B) - misorientation angle is equal to $\pi/4$

where q_1, q_2 are the wave vectors for electron and hole in normal metal with excitation energy E , respectively. k_1 (k_2) and k_3 (k_4) are the wave vectors for electron-like and hole-like quasiparticle corresponding to

inner (outer) Fermi surface in pnictides. Six coefficients a, b, c_1, c_2, d_1, d_2 in Eq. (28) are uniquely determined from six boundary conditions in Eq. (27). Electron and hole coefficients $u_i(k_j)$ and $v_i(k_j)$ in wave functions Eq. (28) are also found from Eq. (A1). The excitation spectrum of a superconducting pnictide, corresponding to a fixed value of $k_y = 0$ at zero angle of misorientation is shown in Fig. 3 (A),(C). The corresponding Fermi surface is shown in Fig. 4. There are four intersection points with $k_y = 0$. At these points, $E(k_x)$ has minima shown in Figs. 3 (A) and (C). The existence of the four quasi-particle states in a pnictide with certain sign of the group velocity follows from Figs. 3 (A) and (C).

The expression for the probability flow with fixed wave vector k_y in the direction parallel to the x axis follows from the BdG equations on sites of the crystal lattice of a pnictide Eq. (A1) and has the following form:

$$\begin{aligned}
J_p = & \frac{2}{\hbar} ((t_1 + 2t_3 \cos k_y) \text{Im}\{(\Psi_{n+1}^\alpha)^* \Psi_n^\alpha - (\bar{\Psi}_{n+1}^\alpha)^* \bar{\Psi}_n^\alpha\} \\
& + (t_2 + 2t_3 \cos k_y) \text{Im}\{(\Psi_{n+1}^\beta)^* \Psi_n^\beta - (\bar{\Psi}_{n+1}^\beta)^* \bar{\Psi}_n^\beta\} \\
& + 4t_4 \sin k_y \text{Re}\{(\Psi_{n+1}^\alpha)^* \Psi_n^\beta + (\Psi_{n+1}^\beta)^* \Psi_n^\alpha \\
& - (\bar{\Psi}_{n+1}^\alpha)^* \bar{\Psi}_n^\beta - (\bar{\Psi}_{n+1}^\beta)^* \bar{\Psi}_n^\alpha\} \\
& + 2\Delta_0 \cos k_y \text{Im}\{(\Psi_{n+1}^\alpha)^* \bar{\Psi}_n^\alpha \\
& + (\bar{\Psi}_{n+1}^\alpha)^* \Psi_n^\alpha + (\Psi_{n+1}^\beta)^* \bar{\Psi}_n^\beta + (\bar{\Psi}_{n+1}^\beta)^* \Psi_n^\beta\}. \quad (29)
\end{aligned}$$

One can show that the boundary conditions Eq. (27) provide the conservation of the probability flow $J = J_p$ across the interface between a normal metal and a superconducting pnictide for each value of k_y . As well as in the case of previously considered 1D model (Eq. (18)), the condition of flow conservation at the NS boundary, having the form of discrete sums (differences) on sites of the crystal lattice (Eqs. (14),(29)), in the case of zero misorientation angle between crystallographic axes of a pnictide and the interface can be written in a quadratic form of the amplitudes of the probability to be in states with quasi-momenta q_1, q_2, k_i , $i = 1..4$ multiplied by group velocities in these states.

The current through the two-dimensional microconstriction between a normal metal and a superconducting pnictide is determined by integration of Eq. (19) over the transverse quasimomentum k_y : $I_p(V) = \eta_2 \int dk_y I(V, k_y)$. In this case the probabilities C, D of the quasiparticle propagation into a superconductor, given by Eqs. (19) and (20), are determined by the sum of the scattering probabilities into individual bands: $C = C_1 + C_2, D = D_1 + D_2$. The coefficients $A, B, C_1, C_2, D_1,$ and D_2 in Eq. (20) are calculated from the boundary conditions Eq. (27) and the expressions of the probability flow in Eqs. (14) and (29). In the actual calculations, one should take into account that the original quasiparticle states should be normalized so that the probability flow in these states, described by the Eqs. (14), (29), is equal to unity.

It is possible to demonstrate, that taking into account oblique hopping between the boundary $\gamma'_1, \gamma'_2, \gamma''_1, \gamma''_2$ (see

Fig. 2) allows to obtain in quasiclassical limit Araújo and Sacramento boundary conditions³³ only for the special case, when the following relations between hopping amplitudes are fulfilled simultaneously:

$$\begin{cases} \gamma_1 = t_1, \\ \gamma_2 = t_2, \\ \gamma'_1 = \gamma'_2 = (t_3 - t_4), \\ \gamma''_1 = \gamma''_2 = (t_3 + t_4). \end{cases} \quad (30)$$

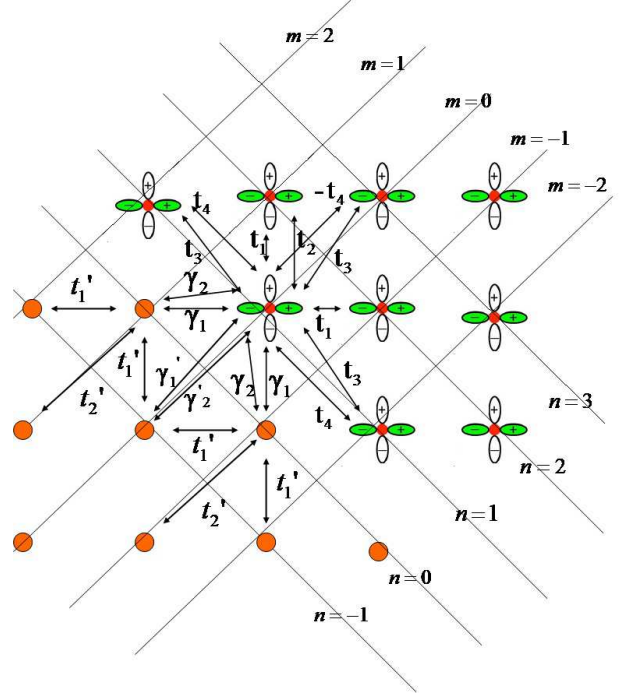


FIG. 5. 2D NS boundary. Angle between crystallographic axes of a pnictide and a normal metal is equal to $\pi/4$. The lower left region (orange circles) corresponds to the region of normal metal with hopping parameters t'_1, t'_2 , right region (sites with two d -orbitals) corresponds to the region of a superconducting pnictide with hopping parameters t_1, t_2, t_3, t_4 . Boundary is described by hopping parameters $\gamma_1, \gamma_2, \gamma'_1, \gamma'_2$.

B. Non-zero misorientation angle

The proposed method allows one to consider the coherent electron transport in NS structures with non-zero misorientation angle as well. It is necessary to note that the microscopic calculation of the conductance for a non-zero misorientation angle of a pnictide crystal with respect to the boundary is presented here for the first time. Previous phenomenological approaches^{33,35} don't allow one to carry out such calculations. In considering the electron transport across NS contact with a nonzero misorientation angle, it is necessary to take into account hopping at the two adjacent atomic layers of a pnictide

(Fig.5). BdG equations in the considered case corresponding to s_{\pm} symmetry of the pair potential in pnictides are given in the Appendix, see Eq. (A2). Hopping across the NS boundary for non-zero misorientation angle is described by a larger number of parameters, rather than at zero misorientation angle between crystallographic axes of a pnictide and the interface (see Fig.5). In addition to hopping parameters γ_1 and γ_2 , we should use additional parameters of hopping across the boundary take into account connection of orbitals from the last atom layer of a pnictide with the penultimate from the boundary atom layer of the normal metal. Taking into account these processes is necessary due to the breaking at the boundary of the diagonal bonds in the crystal lattice of a pnictide for non-zero angle of misorientation (see Fig.5). Also in the normal metal together with the nearest neighbor hopping t'_1 we need to consider the diagonal hopping t'_2 in square lattice.

The wave functions Eq. (A4) and the relation for probability flow (A5) take into account not only the electron transport in two energy bands, but also in two valleys in these bands (see Fig. 3B,D). It is known from the physics of semiconductors, that interference of states in the valleys is possible.⁵⁹ This interference leads to the fact that the condition of flow conservation at the boundary of the NS contact, having the form of discrete sums (differences) on sites of the crystal lattice, in the case of nonzero misorientation angle between crystallographic axes of a pnictide and the interface can not be written in a quadratic form of the amplitudes of the probability to be in states with quasimomentum $q_1, q_2, k_i, i = 1..8$, multiplied by group velocities in these states.

C. Numerical results

Here we will show the results of numerical calculations of angle-resolved conductance (dI/dV) as a function of bias voltage V in normal metal / superconducting pnictide junctions. We use the following values of hopping parameters and chemical potential in a pnictide:

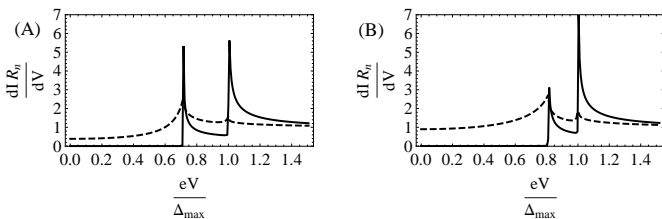


FIG. 6. Angle resolved conductance without misorientation for (A) s_{\pm} -model and (B) s_{++} -model. Value of the quasi-momentum, parallel to the interface, $k_y = 0.01$. The values of hopping parameters at the interface are chosen as $\gamma_1 = 0.1, \gamma_2 = 0.14$ (eV) (dashed line), and $\gamma_1 = 0.009, \gamma_2 = 0.005$ (eV) (solid lines).

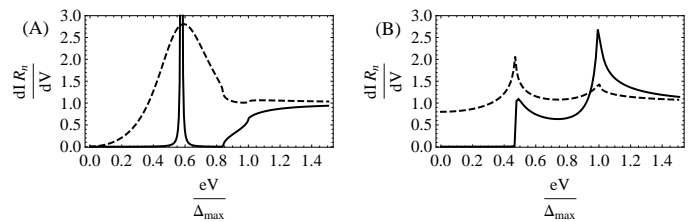


FIG. 7. Same as Fig. 6 but with $k_y = 3\pi/4$.

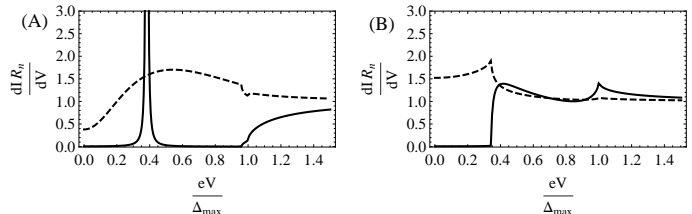


FIG. 8. Same as Fig. 6 but with $k_y = 5\pi/8$

$t_1 = -0.1051, t_2 = 0.1472, t_3 = -0.1909, t_4 = -0.0874$ and $\mu_S = -0.081$ (eV), according to Ref. 23. We assume the momentum dependence of the pair potential in the s_{\pm} model as $\Delta_{\pm}(k) = 4\Delta_0 \cos k_x \cos k_y$ with $\Delta_0 = 0.008$ (eV), and s_{++} model in the form $\Delta = 2\Delta_0(\cos k_x + \cos k_y) + \Delta_1$ with $\Delta_0 = 0.002, \Delta_1 = 0.0042$ (eV). In Figs. 6 to 8, the magnitudes of tunneling conductance normalized by their values in the normal state are shown for s_{\pm} and s_{++} models with zero misorientation angle. The hopping parameters and chemical potential in normal metal are $t'_1 = 0.3, t'_2 = 0, \mu_N = 0.2$. For the hopping parameters at the interface, we choose two cases with $\gamma_1 = 0.009, \gamma_2 = 0.005$ (eV) (low transmissivity) and $\gamma_1 = 0.1, \gamma_2 = 0.14$ (eV) (high transmissivity). Calculated charge conductance dI/dV for low and high transparent junctions with $k_y = 0.01$ is shown in Fig. 6. The horizontal axis represents eV normalized by Δ_{max} , where Δ_{max} is the maximum of two gaps for fixed k_y . One can clearly see two gap features reflecting the presence of two kinds of Fermi surfaces (see Fig. 3) in both s_{\pm} - Fig.6(A) and s_{++} - cases Fig.6(B). In the case of $k_y \sim 0$, the interorbital hopping t_4 is absent. Therefore, the obtained conductance can be represented by a simple summation of the individual orbital's contributions. On the other hand, in the case of s_{\pm} -wave with low transmissive interface, a sharp subgap peak appears in the energy gap as shown in Fig.7(A) and Fig.8(A), respectively. These energy structures do not correspond to the density of states in the bulk. Since dI/dV corresponds to the energy spectrum of local density of states in the low transmissivity, we can conclude that these subgap structures originate from the surface Andreev bound states at finite energies. The bound states disappear in the case of high transparency of the interface. On the other hand, as is seen from Fig.7(B) and Fig.8(B), these features are not present in the case of s_{++} -wave when the signs of pair

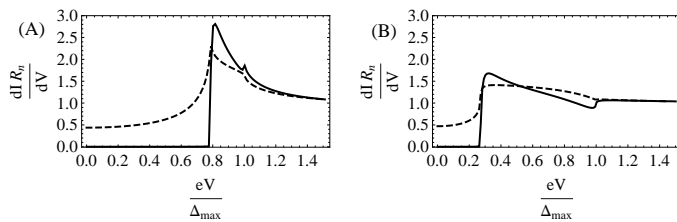


FIG. 9. Angle resolved conductance with misorientation angle $\pi/4$ for (A) s_{\pm} -model and (B) s_{++} -model. Value of the quasimomentum, parallel to the interface, $k_y = 0$. The values of hopping parameters at the interface are chosen as $\gamma_1 = 0.1, \gamma_2 = 0.14, \gamma'_1 = 0.2, \gamma'_2 = 0.06$ (eV) (dashed line), and $\gamma_1 = 0.009, \gamma_2 = 0.005, \gamma'_1 = 0.02, \gamma'_2 = 0.01$ (eV) (solid lines).

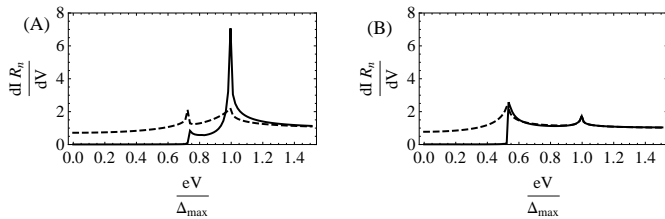


FIG. 10. Same as Fig. 9 but with $k_y = \pi/3$.

potentials in different bands are the same. From these results, we can conclude that the surface Andreev bound states are formed in the s_{\pm} case due to the sign change of pair potential and the interorbital hopping t_4 . Note that a sharp subgap peak in the angle-resolved conductance discussed here should be broadened after summation over k_y is made, as calculated by Onari *et al* within different model.⁴⁸

Next, we calculate the case with finite misorientation angle $\pi/4$. In this case, we shall introduce additional hopping coefficients in a normal metal (t'_2) and at the interface (γ'_1, γ'_2) corresponding to the direction perpendicular to the interface. We choose $t'_2 = 0.01$ (eV), $\gamma'_1 = 0.02, \gamma'_2 = 0.01$ (eV) (low transmissivity case) and $\gamma'_1 = 0.2, \gamma'_2 = 0.06$ (eV) (high transmissivity case). Other hopping parameters are the same as in the case with zero misorientation. In Figs. 9 and 10, we show the angle resolved conductances for $k_y = 0$ and $\pi/3$, respectively. In the case of s_{\pm} model, one can see the two gap features for both $k_y = 0$ and $\pi/3$ as shown in Figs. 9(A) and 10(A). Subgap peaks are absent even in low transparent junctions, in contrast to the case with zero misorientation angle. This is because no sign change at fixed k_y values occurs in the case when misorientation angle equals $\pi/4$ (Fig. 4(B)). For the same reason, gap structure without subgap peaks appears also in the case of s_{++} model.

Let us summarize the results of the conductance of normal metal / superconducting pnictide junctions. In the case of s_{++} model, only the two-gap structure with-

out subgap peaks appears for any misorientation angle and any value of k_y . On the other hand, in the case of s_{\pm} model with low transparent interface, subgap peaks appear for zero misorientation angle and finite k_y . These subgap peaks originate from sign change of the pair potential at fixed k_y values in the presence of the interorbital hopping.

V. CONCLUSION

In this paper, we have presented consistent tight-binding model for the coherent electronic transport in the contact between a normal metal and a superconductor. Based on a tight-binding model beyond effective mass approximation, we have derived boundary conditions on a wave function at a contact between a normal metal and a superconductor with unconventional pairing symmetry. We have extended the previous tight-binding approach used in semiconducting heterostructures⁴⁹ to the case of superconducting junctions. The obtained boundary conditions contain real space information only without any momentum derivatives, and they have clear physical meaning. These conditions provide current conservation and enable one to formulate consistent approach for tunneling spectroscopy of superconductors with complex nonparabolic energy spectrum, including multiband electronic structure and unconventional symmetry of superconducting pairing. We have shown that application of this theory to single-band superconductor junctions allows one to reproduce the preexisting conductance formula 6. Based on the derived boundary conditions, we have calculated conductance in normal metal / superconducting pnictide junctions for different misorientation angles between the interface and the crystallographic axes of a pnictide. The present approach provides the basis for tunneling spectroscopy of multi-orbital superconductors. Moreover, this approach is suitable for a consistent description of electronic transport in structures with surface states described by Majorana fermions in topological superconductors,^{56,60-75} which would be the subject of our future study.

ACKNOWLEDGMENTS

We gratefully acknowledge M.Yu. Kupriyanov, I.I. Mazin, A. S. Melnikov and S. Onari for valuable discussions. This work was supported in part by a Grant-in Aid for Scientific Research from MEXT of Japan, "Topological Quantum Phenomena" Grants No. 22103005 and No. 20654030 (Y.T.), RFBR Grant 11-02-12084-ofi-m-2011, Dutch Foundation for Fundamental Research on Matter (FOM) and by EU-Japan program "IRON SEA".

Appendix A: Derivation of equations of two-dimensional model

Bogoliubov-de Gennes equations on sites of the Fe crystal lattice in the $x - y$ plane of a pnictide for the case of

zero misorientation angle of the crystallographic axes of pnictides with respect to the interface have the following form:

$$\left\{ \begin{array}{l}
 t_1(\Psi_{n+1,m}^\alpha + \Psi_{n-1,m}^\alpha) + t_2(\Psi_{n,m+1}^\alpha + \Psi_{n,m-1}^\alpha) \\
 + t_3(\Psi_{n+1,m+1}^\alpha + \Psi_{n-1,m-1}^\alpha + \Psi_{n+1,m-1}^\alpha \\
 + \Psi_{n-1,m+1}^\alpha) + t_4(-\Psi_{n+1,m+1}^\beta - \Psi_{n-1,m-1}^\beta \\
 + \Psi_{n+1,m-1}^\beta + \Psi_{n-1,m+1}^\beta) - \mu_S \bar{\Psi}_{n,m}^\alpha + \Delta_0(\bar{\Psi}_{n+1,m+1}^\alpha \\
 + \bar{\Psi}_{n-1,m-1}^\alpha + \bar{\Psi}_{n+1,m-1}^\alpha + \bar{\Psi}_{n-1,m+1}^\alpha) = \varepsilon \Psi_{n,m}^\alpha, \\
 t_2(\Psi_{n+1,m}^\beta + \Psi_{n-1,m}^\beta) + t_1(\Psi_{n,m+1}^\beta + \Psi_{n,m-1}^\beta) \\
 + t_3(\Psi_{n+1,m+1}^\beta + \Psi_{n-1,m-1}^\beta + \Psi_{n+1,m-1}^\beta \\
 + \Psi_{n-1,m+1}^\beta) + t_4(-\Psi_{n+1,m+1}^\alpha - \Psi_{n-1,m-1}^\alpha \\
 + \Psi_{n+1,m-1}^\alpha + \Psi_{n-1,m+1}^\alpha) - \mu_S \bar{\Psi}_{n,m}^\beta + \Delta_0(\bar{\Psi}_{n+1,m+1}^\beta \\
 + \bar{\Psi}_{n-1,m-1}^\beta + \bar{\Psi}_{n+1,m-1}^\beta + \bar{\Psi}_{n-1,m+1}^\beta) = \varepsilon \Psi_{n,m}^\beta, \\
 t_1(\bar{\Psi}_{n+1,m}^\alpha + \bar{\Psi}_{n-1,m}^\alpha) + t_2(\bar{\Psi}_{n,m+1}^\alpha + \bar{\Psi}_{n,m-1}^\alpha) \\
 + t_3(\bar{\Psi}_{n+1,m+1}^\alpha + \bar{\Psi}_{n-1,m-1}^\alpha + \bar{\Psi}_{n+1,m-1}^\alpha \\
 + \bar{\Psi}_{n-1,m+1}^\alpha) + t_4(-\bar{\Psi}_{n+1,m+1}^\beta - \bar{\Psi}_{n-1,m-1}^\beta \\
 + \bar{\Psi}_{n+1,m-1}^\beta + \bar{\Psi}_{n-1,m+1}^\beta) - \mu_S \bar{\Psi}_{n,m}^\alpha - \Delta_0(\Psi_{n+1,m+1}^\alpha \\
 + \Psi_{n-1,m-1}^\alpha + \Psi_{n+1,m-1}^\alpha + \Psi_{n-1,m+1}^\alpha) = -\varepsilon \bar{\Psi}_{n,m}^\alpha, \\
 t_2(\bar{\Psi}_{n+1,m}^\beta + \bar{\Psi}_{n-1,m}^\beta) + t_1(\bar{\Psi}_{n,m+1}^\beta + \bar{\Psi}_{n,m-1}^\beta) \\
 + t_3(\bar{\Psi}_{n+1,m+1}^\beta + \bar{\Psi}_{n-1,m-1}^\beta + \bar{\Psi}_{n+1,m-1}^\beta \\
 + \bar{\Psi}_{n-1,m+1}^\beta) + t_4(-\bar{\Psi}_{n+1,m+1}^\alpha - \bar{\Psi}_{n-1,m-1}^\alpha \\
 + \bar{\Psi}_{n+1,m-1}^\alpha + \bar{\Psi}_{n-1,m+1}^\alpha) - \mu_S \bar{\Psi}_{n,m}^\beta - \Delta_0(\Psi_{n+1,m+1}^\beta \\
 + \Psi_{n-1,m-1}^\beta + \Psi_{n+1,m-1}^\beta + \Psi_{n-1,m+1}^\beta) = -\varepsilon \bar{\Psi}_{n,m}^\beta,
 \end{array} \right. \tag{A1}$$

where t_i , $i = 1..4$, are hopping amplitudes between orbitals on sites in a pnictide in the two-orbital model.⁵⁷ The value of Δ_0 is the amplitude of the anisotropic pair potential corresponding to the considered s_\pm superconducting pairing model: $\Delta_\pm(k) = 4\Delta_0 \cos k_x \cos k_y$,⁵⁸ k_y , k_x are parallel and perpendicular to the interface components of quasimomentum respectively. The wave functions of a superconducting pnictide have the upper orbital index $\alpha(\beta)$: $\Psi_i^{\alpha(\beta)}$, corresponding to $d_{xz}(d_{yz})$ orbital respectively. The subscripts n, m of the wave function $\Psi_{n,m}^{\alpha(\beta)}$ of a pnictide describe the coordinates of sites of the crystal lattice (Fig. 2). As well as in the considered above 1D-model $\Psi_{n,m}^{\alpha(\beta)}$ in Eq. (A1) describe the electron states, and $\bar{\Psi}_{n,m}^{\alpha(\beta)}$ - hole states.

For misorientation angle $\pi/4$ between crystallographic axes of a pnictide and the interface (Fig.5), Bogoliubov-de Gennes equations on sites of the Fe crystal lattice in

the $x - y$ plane of a pnictide differ from Eq. (A1) and have the following form:

$$\left\{ \begin{array}{l}
-\mu_S \Psi_{n,m}^\alpha + t_1(\Psi_{n+1,m-1}^\alpha + \Psi_{n-1,m+1}^\alpha) \\
+ t_2(\Psi_{n+1,m+1}^\alpha + \Psi_{n-1,m-1}^\alpha) \\
+ t_3(\Psi_{n+2,m}^\alpha + \Psi_{n-2,m}^\alpha + \Psi_{n,m-2}^\alpha + \Psi_{n,m+2}^\alpha) \\
+ t_4(-\Psi_{n+2,m}^\beta - \Psi_{n-2,m}^\beta + \Psi_{n,m-2}^\beta + \Psi_{n,m+2}^\beta) \\
+ \Delta_0(\bar{\Psi}_{n+2,m}^\alpha + \bar{\Psi}_{n-2,m}^\alpha + \bar{\Psi}_{n,m-2}^\alpha + \bar{\Psi}_{n,m+2}^\alpha) \\
= \varepsilon \Psi_{n,m}^\alpha, \\
-\mu_S \Psi_{n,m}^\beta + t_2(\Psi_{n+1,m-1}^\beta + \Psi_{n-1,m+1}^\beta) \\
+ t_1(\Psi_{n+1,m+1}^\beta + \Psi_{n-1,m-1}^\beta) \\
+ t_3(\Psi_{n+2,m}^\beta + \Psi_{n-2,m}^\beta + \Psi_{n,m-2}^\beta + \Psi_{n,m+2}^\beta) \\
+ t_4(-\Psi_{n+2,m}^\alpha - \Psi_{n-2,m}^\alpha + \Psi_{n,m-2}^\alpha + \Psi_{n,m+2}^\alpha) \\
+ \Delta_0(\bar{\Psi}_{n+2,m}^\beta + \bar{\Psi}_{n-2,m}^\beta + \bar{\Psi}_{n,m-2}^\beta + \bar{\Psi}_{n,m+2}^\beta) \\
= \varepsilon \Psi_{n,m}^\beta, \\
-\mu_S \bar{\Psi}_{n,m}^\alpha + t_1(\bar{\Psi}_{n+1,m-1}^\alpha + \bar{\Psi}_{n-1,m+1}^\alpha) \\
+ t_2(\bar{\Psi}_{n+1,m+1}^\alpha + \bar{\Psi}_{n-1,m-1}^\alpha) \\
+ t_3(\bar{\Psi}_{n+2,m}^\alpha + \bar{\Psi}_{n-2,m}^\alpha + \bar{\Psi}_{n,m-2}^\alpha + \bar{\Psi}_{n,m+2}^\alpha) \\
+ t_4(-\bar{\Psi}_{n+2,m}^\beta - \bar{\Psi}_{n-2,m}^\beta + \bar{\Psi}_{n,m-2}^\beta + \bar{\Psi}_{n,m+2}^\beta) \\
- \Delta_0(\Psi_{n+2,m}^\alpha + \Psi_{n-2,m}^\alpha + \Psi_{n,m-2}^\alpha + \Psi_{n,m+2}^\alpha) \\
= -\varepsilon \bar{\Psi}_{n,m}^\alpha, \\
-\mu_S \bar{\Psi}_{n,m}^\beta + t_2(\bar{\Psi}_{n+1,m-1}^\beta + \bar{\Psi}_{n-1,m+1}^\beta) \\
+ t_2(\bar{\Psi}_{n+1,m+1}^\beta + \bar{\Psi}_{n-1,m-1}^\beta) \\
+ t_3(\bar{\Psi}_{n+2,m}^\beta + \bar{\Psi}_{n-2,m}^\beta + \bar{\Psi}_{n,m-2}^\beta + \bar{\Psi}_{n,m+2}^\beta) \\
+ t_4(-\bar{\Psi}_{n+2,m}^\alpha - \bar{\Psi}_{n-2,m}^\alpha + \bar{\Psi}_{n,m-2}^\alpha + \bar{\Psi}_{n,m+2}^\alpha) \\
- \Delta_0(\Psi_{n+2,m}^\beta + \Psi_{n-2,m}^\beta + \Psi_{n,m-2}^\beta + \Psi_{n,m+2}^\beta) \\
= -\varepsilon \bar{\Psi}_{n,m}^\beta.
\end{array} \right. \quad (A2)$$

The boundary conditions for the contact between a normal metal and a pnictide, considered in the framework of the two-orbital model, for misorientation angle $\pi/4$ between crystallographic axes of a pnictide and the interface have the following form:

$$\left\{ \begin{array}{l}
t'_1 \Phi_1(e^{ik_y l} + e^{-ik_y l}) + t'_2 \Phi_2 = \Psi_1^\alpha(\gamma_1 e^{ik_y l} + \gamma_2 e^{-ik_y l}) \\
+ \Psi_1^\beta(\gamma_1 e^{-ik_y l} + \gamma_2 e^{ik_y l}) + \gamma'_1 \Psi_2^\alpha + \gamma'_2 \Psi_2^\beta, \\
t'_1 \bar{\Phi}_1(e^{ik_y l} + e^{-ik_y l}) + t'_2 \bar{\Phi}_2 = \bar{\Psi}_1^\alpha(\gamma_1 e^{ik_y l} + \gamma_2 e^{-ik_y l}) \\
+ \bar{\Psi}_1^\beta(\gamma_1 e^{-ik_y l} + \gamma_2 e^{-ik_y l}) + \gamma'_1 \bar{\Psi}_2^\alpha + \gamma'_2 \bar{\Psi}_2^\beta, \\
\Phi_0(\gamma_1 e^{ik_y l} + \gamma_2 e^{-ik_y l}) + \gamma'_1 \Phi_{-1} = t_1 \Psi_0^\alpha e^{ik_y l} \\
+ t_2 \Psi_0^\beta e^{-ik_y l} + t_3 \Psi_{-1}^\alpha - t_4 \Psi_{-1}^\beta + \Delta_0 \bar{\Psi}_{-1}^\alpha, \\
\bar{\Phi}_0(\gamma_1 e^{ik_y l} + \gamma_2 e^{-ik_y l}) + \gamma'_1 \bar{\Phi}_{-1} = t_1 \bar{\Psi}_0^\alpha e^{ik_y l} \\
+ t_2 \bar{\Psi}_0^\beta e^{-ik_y l} + t_3 \bar{\Psi}_{-1}^\alpha - t_4 \bar{\Psi}_{-1}^\beta - \Delta_0 \Psi_{-1}^\alpha, \\
\Phi_0(\gamma_1 e^{-ik_y l} + \gamma_2 e^{ik_y l}) + \gamma'_2 \Phi_{-1} = t_1 \Psi_0^\beta e^{ik_y l} \\
+ t_2 \Psi_0^\alpha e^{-ik_y l} + t_3 \Psi_{-1}^\beta - t_4 \Psi_{-1}^\alpha + \Delta_0 \bar{\Psi}_{-1}^\beta, \\
\bar{\Phi}_0(\gamma_1 e^{-ik_y l} + \gamma_2 e^{ik_y l}) + \gamma'_2 \bar{\Phi}_{-1} = t_1 \bar{\Psi}_0^\beta e^{ik_y l} \\
+ t_2 \bar{\Psi}_0^\alpha e^{-ik_y l} + t_3 \bar{\Psi}_{-1}^\beta - t_4 \bar{\Psi}_{-1}^\alpha - \Delta_0 \Psi_{-1}^\beta, \\
\gamma'_1 \Phi_0 = t_3 \Psi_0^\alpha - t_4 \Psi_0^\beta + \Delta_0 \bar{\Psi}_0^\alpha, \\
\gamma'_1 \bar{\Phi}_0 = t_3 \bar{\Psi}_0^\alpha - t_4 \bar{\Psi}_0^\beta - \Delta_0 \Psi_0^\alpha, \\
\gamma'_2 \Phi_0 = t_3 \Psi_0^\beta - t_4 \Psi_0^\alpha + \Delta_0 \bar{\Psi}_0^\beta, \\
\gamma'_2 \bar{\Phi}_0 = t_3 \bar{\Psi}_0^\beta - t_4 \bar{\Psi}_0^\alpha - \Delta_0 \Psi_0^\beta, \\
t'_2 \Phi_1 = \gamma'_1 \Psi_1^\alpha + \gamma'_2 \Psi_1^\beta, \\
t'_2 \bar{\Phi}_1 = \gamma'_1 \bar{\Psi}_1^\alpha + \gamma'_2 \bar{\Psi}_1^\beta.
\end{array} \right. \quad (A3)$$

As in the previously considered case of boundary conditions for zero misorientation angle Eq. (27), due to translational symmetry in the direction parallel to the boundary, in electron (hole) wave functions $\Psi_{n,m}^{\alpha(\beta)}$ ($\bar{\Psi}_{n,m}^{\alpha(\beta)}$) second subscript (m) corresponding to the coordinate of an atom in a direction parallel to the boundary is omitted.

The wave functions in a normal metal / superconducting pnictide contact in the case of misorientation angle $\pi/4$ between crystallographic axes of a pnictide and the interface are defined by eight plane waves with amplitudes $a_1, b_1, a_2, b_2, c_1, c_2, d_1, d_2, f_1, f_2, g_1, g_2$. Here the coefficients a_1, b_1, a_2, b_2 describe Andreev and normal reflected waves, while $c_1, c_2, d_1, d_2, f_1, f_2, g_1, g_2$ describe eight waves transmitted into a two-band superconducting pnictide:

$$\left\{ \begin{array}{l}
\Phi_n = \exp(iq_1nl) + b_1 \exp(-iq_1nl) + b_2 \exp(-iq_2nl), \\
\bar{\Phi}_n = a_1 \exp(iq_3nl) + a_2 \exp(iq_4nl), \\
\Psi_n^\alpha = c_1 u_1(k_1) \exp(ik_1nl) + c_2 u_1(k_2) \exp(ik_2nl) \\
+ d_1 u_1(k_3) \exp(ik_3nl) + d_2 u_1(k_4) \exp(ik_4nl) \\
+ f_1 u_1(k_5) \exp(ik_5nl) + f_2 u_1(k_6) \exp(ik_6nl) \\
+ g_1 u_1(k_7) \exp(ik_7nl) + g_2 u_1(k_8) \exp(ik_8nl), \\
\Psi_n^\beta = c_1 u_2(k_1) \exp(ik_1nl) + c_2 u_2(k_2) \exp(ik_2nl) \\
+ d_1 u_2(k_3) \exp(ik_3nl) + d_2 u_2(k_4) \exp(ik_4nl) \\
+ f_1 u_2(k_5) \exp(ik_5nl) + f_2 u_2(k_6) \exp(ik_6nl) \\
+ g_1 u_2(k_7) \exp(ik_7nl) + g_2 u_2(k_8) \exp(ik_8nl), \\
\bar{\Psi}_n^\alpha = c_1 v_1(k_1) \exp(ik_1nl) + c_2 v_1(k_2) \exp(ik_2nl) \\
+ d_1 v_1(k_3) \exp(ik_3nl) + d_2 v_1(k_4) \exp(ik_4nl) \\
+ f_1 v_1(k_5) \exp(ik_5nl) + f_2 v_1(k_6) \exp(ik_6nl) \\
+ g_1 v_1(k_7) \exp(ik_7nl) + g_2 v_1(k_8) \exp(ik_8nl), \\
\bar{\Psi}_n^\beta = c_1 v_2(k_1) \exp(ik_1nl) + c_2 v_2(k_2) \exp(ik_2nl) \\
+ d_1 v_2(k_3) \exp(ik_3nl) + d_2 v_2(k_4) \exp(ik_4nl) \\
+ f_1 v_2(k_5) \exp(ik_5nl) + f_2 v_2(k_6) \exp(ik_6nl) \\
+ g_1 v_2(k_7) \exp(ik_7nl) + g_2 v_2(k_8) \exp(ik_8nl).
\end{array} \right. \quad (\text{A4})$$

Four transmitted waves with amplitudes c_1, c_2, d_1, d_2 correspond to the lower band, depicted by black solid line on Fig. 3(B),(D). These four waves are propagating waves except the energy range lower than the superconducting gap Δ_0 . Four plane waves with amplitudes f_1, f_2, g_1, g_2 correspond to the upper band, depicted by red dashed line on Fig. 3(B),(D). These four waves are evanescent

waves on the scale of pair potential Δ_0 .

Expression for the probability flow in the case of misorientation angle between crystallographic axes of a pnictide and the interface equal to $\pi/4$ differs from the corresponding relation for the case of zero misorientation angle Eq. (29) and has the following form:

$$\begin{aligned}
J = & \frac{2}{\hbar} (t_1 \text{Im}\{(\Psi_{n+1}^\alpha)^* \Psi_n^\alpha e^{ik_y l}\} \\
& + t_2 \text{Im}\{(\Psi_{n+1}^\alpha)^* \Psi_n^\alpha e^{-ik_y l}\} \\
& + t_3 \text{Im}\{(\Psi_{n+1}^\alpha)^* \Psi_{n-1}^\alpha + (\Psi_{n+2}^\alpha)^* \Psi_n^\alpha\} \\
& + t_1 \text{Im}\{(\Psi_{n+1}^\beta)^* \Psi_n^\beta e^{-ik_y l}\} + t_2 \text{Im}\{(\Psi_{n+1}^\beta)^* \Psi_n^\beta e^{ik_y l}\} \\
& + t_3 \text{Im}\{(\Psi_{n+1}^\beta)^* \Psi_{n-1}^\beta + (\Psi_{n+2}^\beta)^* \Psi_n^\beta\} \\
& - t_4 (\text{Im}\{(\Psi_{n+1}^\alpha)^* \Psi_{n-1}^\beta\} + \text{Im}\{(\Psi_{n+1}^\beta)^* \Psi_{n-1}^\alpha\}) \\
& + \text{Im}\{(\Psi_{n+2}^\alpha)^* \Psi_n^\beta\} + \text{Im}\{(\Psi_{n+2}^\beta)^* \Psi_n^\alpha\}) \\
& - t_1 \text{Im}\{(\bar{\Psi}_{n+1}^\alpha)^* \bar{\Psi}_n^\alpha e^{ik_y l}\} - t_2 \text{Im}\{(\bar{\Psi}_{n+1}^\alpha)^* \bar{\Psi}_n^\alpha e^{-ik_y l}\} \\
& - t_3 \text{Im}\{(\bar{\Psi}_{n+1}^\alpha)^* \bar{\Psi}_{n-1}^\alpha + (\bar{\Psi}_{n+2}^\alpha)^* \bar{\Psi}_n^\alpha\} \\
& - t_1 \text{Im}\{(\bar{\Psi}_{n+1}^\beta)^* \bar{\Psi}_n^\beta e^{-ik_y l}\} - t_2 \text{Im}\{(\bar{\Psi}_{n+1}^\beta)^* \bar{\Psi}_n^\beta e^{ik_y l}\} \\
& - t_3 \text{Im}\{(\bar{\Psi}_{n+1}^\beta)^* \bar{\Psi}_{n-1}^\beta + (\bar{\Psi}_{n+2}^\beta)^* \bar{\Psi}_n^\beta\} \\
& + t_4 (\text{Im}\{(\bar{\Psi}_{n+1}^\alpha)^* \bar{\Psi}_{n-1}^\beta\} + \text{Im}\{(\bar{\Psi}_{n+1}^\beta)^* \bar{\Psi}_{n-1}^\alpha\}) \\
& + \text{Im}\{(\bar{\Psi}_{n+2}^\alpha)^* \bar{\Psi}_n^\beta\} + \text{Im}\{(\bar{\Psi}_{n+2}^\beta)^* \bar{\Psi}_n^\alpha\}) \\
& + \Delta_0 \text{Im}\{(\Psi_{n+1}^\alpha)^* \bar{\Psi}_{n-1}^\alpha + (\bar{\Psi}_{n+1}^\alpha)^* \Psi_{n-1}^\alpha \\
& + (\Psi_{n+1}^\beta)^* \bar{\Psi}_{n-1}^\beta + (\bar{\Psi}_{n+1}^\beta)^* \Psi_{n-1}^\beta + (\Psi_{n+2}^\alpha)^* \bar{\Psi}_n^\alpha \\
& + (\bar{\Psi}_{n+2}^\alpha)^* \Psi_n^\alpha + (\Psi_{n+2}^\beta)^* \bar{\Psi}_n^\beta + (\bar{\Psi}_{n+2}^\beta)^* \Psi_n^\beta\}. \quad (\text{A5})
\end{aligned}$$

* igor-devyatov@yandex.ru

- ¹ E. L. Wolf, *Principles of electron tunneling spectroscopy* (Oxford University Press, Oxford, 1985).
- ² J. Bardeen, Phys. Rev. Lett. **6**, 57 (1961).
- ³ M. H. Cohen, L. M. Falicov, and J. C. Phillips, Phys. Rev. Lett. **8**, 316 (1962).
- ⁴ G. E. Blonder, M. Tinkham, and T. M. Klapwijk, Phys. Rev. B **25**, 4515 (1982).
- ⁵ C. Bruder, Phys. Rev. B **41**, 4017 (1990).
- ⁶ Y. Tanaka and S. Kashiwaya, Phys. Rev. Lett. **74**, 3451 (1995).
- ⁷ S. Kashiwaya and Y. Tanaka, Rep. Prog. Phys. **63**, 1641 (2000).
- ⁸ C.-R. Hu, Phys. Rev. Lett. **72**, 1526 (1994).
- ⁹ T. Löfwander, V. S. Shumeiko, and G. Wendin, Superconductor Science and Technology **14**, 53 (2001).
- ¹⁰ Y. Tanaka and S. Kashiwaya, Phys. Rev. B **53**, R11957 (1996).
- ¹¹ Y. S. Barash, H. Burkhardt, and D. Rainer, Phys. Rev. Lett. **77**, 4070 (1996).
- ¹² Y. Tanaka and S. Kashiwaya, Phys. Rev. B **56**, 892 (1997).
- ¹³ M. Yamashiro, Y. Tanaka, and S. Kashiwaya, Phys. Rev. B **56**, 7847 (1997).
- ¹⁴ M. Yamashiro, Y. Tanaka, Y. Tanuma, and S. Kashiwaya, J. Phys. Soc. Jpn. **67**, 3224 (1998).
- ¹⁵ C. Honerkamp and M. Sigrist, Journal of Low Temperature Physics **111**, 895 (1998), 10.1023/A:1022281409397.
- ¹⁶ A. P. Mackenzie and Y. Maeno, Rev. Mod. Phys. **75**, 657 (2003).
- ¹⁷ M. Matsumoto and M. Sigrist, J. Phys. Soc. Jpn. **68**, 994 (1999).
- ¹⁸ A. Furusaki, M. Matsumoto, and M. Sigrist, Phys. Rev. B **64**, 054514 (2001).
- ¹⁹ S. Kashiwaya, H. Kashiwaya, H. Kambara, T. Furuta, H. Yaguchi, Y. Tanaka, and Y. Maeno, Phys. Rev. Lett. **107**, 077003 (2011).
- ²⁰ I. I. Mazin, D. J. Singh, M. D. Johannes, and M. H. Du, Phys. Rev. Lett. **101**, 057003 (2008).
- ²¹ K. Kuroki, S. Onari, R. Arita, H. Usui, Y. Tanaka, H. Kontani, and H. Aoki, Phys. Rev. Lett. **101**, 087004 (2008).
- ²² H. Kontani and S. Onari, Phys. Rev. Lett. **104**, 157001 (2010).
- ²³ A. Moreo, M. Daghofer, J. A. Riera, and E. Dagotto, Phys. Rev. B **79**, 134502 (2009).
- ²⁴ Y. S. Hor, A. J. Williams, J. G. Checkelsky, P. Roushan, J. Seo, Q. Xu, H. W. Zandbergen, A. Yazdani, N. P. Ong,

- and R. J. Cava, Phys. Rev. Lett. **104**, 057001 (2010).
- ²⁵ S. Sasaki, M. Kriener, K. Segawa, K. Yada, Y. Tanaka, M. Sato, and Y. Ando, Phys. Rev. Lett. **107**, 217001 (2011).
- ²⁶ G. Koren, T. Kirzhner, E. Lahoud, K. B. Chashka, and A. Kanigel, Phys. Rev. B **84**, 224521 (2011).
- ²⁷ T. Kirzhner, E. Lahoud, K. B. Chaska, Z. Salman, and A. Kanigel, Phys. Rev. B **86**, 064517 (2012).
- ²⁸ F. Yang, Y. Ding, F. Qu, J. Shen, J. Chen, Z. Wei, Z. Ji, G. Liu, J. Fan, C. Yang, T. Xiang, and L. Lu, Phys. Rev. B **85**, 104508 (2012).
- ²⁹ L. Fu and E. Berg, Phys. Rev. Lett. **105**, 097001 (2010).
- ³⁰ L. Hao and T. K. Lee, Phys. Rev. B **83**, 134516 (2011).
- ³¹ T. H. Hsieh and L. Fu, Phys. Rev. Lett. **108**, 107005 (2012).
- ³² A. Yamakage, K. Yada, M. Sato, and Y. Tanaka, Phys. Rev. B **85**, 180509 (2012).
- ³³ M. A. N. Araújo and P. D. Sacramento, Phys. Rev. B **79**, 174529 (2009).
- ³⁴ A. V. Burmistrova and I. A. Devyatov, JETP Letters **95**, 263 (2012).
- ³⁵ I. B. Sperstad, J. Linder, and A. Sudbø, Phys. Rev. B **80**, 144507 (2009).
- ³⁶ A. A. Golubov, A. Brinkman, Y. Tanaka, I. I. Mazin, and O. V. Dolgov, Phys. Rev. Lett. **103**, 077003 (2009).
- ³⁷ I. A. Devyatov, M. Y. Romashka, and A. V. Burmistrova, JETP Letters **91**, 297 (2010).
- ³⁸ A. V. Burmistrova, T. Y. Karminskaya, and I. A. Devyatov, JETP Letters **93**, 133 (2011).
- ³⁹ A. V. Burmistrova, I. A. Devyatov, M. Y. Kupriyanov, and T. Y. Karminskaya, JETP Letters **93**, 203 (2011).
- ⁴⁰ W.-Q. Chen, F. Ma, Z.-Y. Lu, and F.-C. Zhang, Phys. Rev. Lett. **103**, 207001 (2009).
- ⁴¹ E. Berg, N. H. Lindner, and T. Pereg-Barnea, Phys. Rev. Lett. **106**, 147003 (2011).
- ⁴² Y. Tanuma, Y. Tanaka, M. Yamashiro, and S. Kashiwaya, Phys. Rev. B **57**, 7997 (1998).
- ⁴³ Y. Tanuma, Y. Tanaka, M. Yamashiro, and S. Kashiwaya, J. Phys. Soc. Jpn. **67**, 1118 (1998).
- ⁴⁴ Y. Tanuma, Y. Tanaka, M. Ogata, and S. Kashiwaya, Phys. Rev. B **60**, 9817 (1999).
- ⁴⁵ Y. Tanuma, K. Kuroki, Y. Tanaka, and S. Kashiwaya, Phys. Rev. B **64**, 214510 (2001).
- ⁴⁶ Y. Tanuma, K. Kuroki, Y. Tanaka, R. Arita, S. Kashiwaya, and H. Aoki, Phys. Rev. B **66**, 094507 (2002).
- ⁴⁷ Y. Tanuma, K. Kuroki, Y. Tanaka, and S. Kashiwaya, Phys. Rev. B **68**, 214513 (2003).
- ⁴⁸ S. Onari and Y. Tanaka, Phys. Rev. B **79**, 174526 (2009).
- ⁴⁹ Q.-G. Zhu and H. Kroemer, Phys. Rev. B **27**, 3519 (1983).
- ⁵⁰ A. V. Burmistrova and I. A. Devyatov, Pis'ma v ZETF **96**, 430 (2012).
- ⁵¹ M. Tinkham, *Introduction to Superconductivity* (McGraw-Hill book company, New York, 1975).
- ⁵² B. Laikhtman, Phys. Rev. B **46**, 4769 (1992).
- ⁵³ W. A. Harrison, Phys. Rev. **123**, 85 (1961).
- ⁵⁴ S. Kashiwaya, Y. Tanaka, M. Koyanagi, and K. Kajimura, Phys. Rev. B **53**, 2667 (1996).
- ⁵⁵ M. Sato, Y. Tanaka, K. Yada, and T. Yokoyama, Phys. Rev. B **83**, 224511 (2011).
- ⁵⁶ Y. Tanaka, M. Sato, and N. Nagaosa, J. Phys. Soc. Jpn. **81**, 011013 (2012).
- ⁵⁷ S. Raghu, X.-L. Qi, C.-X. Liu, D. J. Scalapino, and S.-C. Zhang, Phys. Rev. B **77**, 220503 (2008).
- ⁵⁸ M. M. Korshunov and I. Eremin, Phys. Rev. B **78**, 140509 (2008).
- ⁵⁹ T. Ando and H. Akera, Phys. Rev. B **40**, 11619 (1989).
- ⁶⁰ L. Fu and C. L. Kane, Phys. Rev. Lett. **100**, 096407 (2008).
- ⁶¹ L. Fu and C. L. Kane, Phys. Rev. Lett. **102**, 216403 (2009).
- ⁶² A. R. Akhmerov, J. Nilsson, and C. W. J. Beenakker, Phys. Rev. Lett. **102**, 216404 (2009).
- ⁶³ K. T. Law, P. A. Lee, and T. K. Ng, Phys. Rev. Lett. **103**, 237001 (2009).
- ⁶⁴ J. Linder, Y. Tanaka, T. Yokoyama, A. Sudbo, and N. Nagaosa, Phys. Rev. Lett. **104**, 067001 (2010).
- ⁶⁵ Y. Tanaka, T. Yokoyama, and N. Nagaosa, Phys. Rev. Lett. **103**, 107002 (2009).
- ⁶⁶ M. Sato and S. Fujimoto, Phys. Rev. B **79**, 094504 (2009).
- ⁶⁷ T. Yokoyama, Phys. Rev. B **86**, 075410 (2012).
- ⁶⁸ J. Alicea, Phys. Rev. B **81**, 125318 (2010).
- ⁶⁹ Y. Oreg, G. Refael, and F. von Oppen, Phys. Rev. Lett. **105**, 177002 (2010).
- ⁷⁰ R. M. Lutchyn, J. D. Sau, and S. Das Sarma, Phys. Rev. Lett. **105**, 077001 (2010).
- ⁷¹ P. A. Ioselevich and M. V. Feigel'man, Phys. Rev. Lett. **106**, 077003 (2011).
- ⁷² A. Yamakage, Y. Tanaka, and N. Nagaosa, Phys. Rev. Lett. **108**, 087003 (2012).
- ⁷³ Y. Tanaka, T. Yokoyama, A. V. Balatsky, and N. Nagaosa, Phys. Rev. B **79**, 060505 (2009).
- ⁷⁴ Y. Tanaka, Y. Mizuno, T. Yokoyama, K. Yada, and M. Sato, Phys. Rev. Lett. **105**, 097002 (2010).
- ⁷⁵ K. Yada, M. Sato, Y. Tanaka, and T. Yokoyama, Phys. Rev. B **83**, 064505 (2011).